ELSEVIER

Thermochimica Acta 399 (2003) 153–165

thermochimica acta

www.elsevier.com/locate/tca

Studies on energetic compounds part 28: thermolysis of HMX and its plastic bonded explosives containing Estane

Gurdip Singh [a,*], S. Prem Felix [a], Pramod Soni [b]

[a] *Department of Chemistry, DDU Gorakhpur University, Gorakhpur 273 009, Uttar Pradesh, India*
[b] *Terminal Ballistic Research Laboratory, Sector 30, Chandigarh, Punjab, India*

Received 9 April 2002; received in revised form 30 June 2002; accepted 9 August 2002

Abstract

The thermolysis of HMX, Estane and two of their plastic bonded explosives (PBXs) namely HXE 9505 and HXE 9010 were investigated using non-isothermal TG–DTG and DSC under an inert gas (N_2) atmosphere. Non-isothermal TG, isothermal TG and DTA were also undertaken in air atmosphere on the above-said samples. Lowering of decomposition temperature of HMX has been observed when Estane was coated over it, to make their PBXs. The extent of lowering was increased as the amount of Estane increased in the PBX. Kinetic analyses of isothermal TG data has been made by using model fitting methods as well as by using a model free isoconversional method. The merits and demerits of both modes of kinetic analysis have been critically evaluated by making use of the kinetic parameters obtained there from to explain the thermal characteristics of the samples studied. Explosion delay measurements have been made on HMX and its PBXs and the kinetic parameters were also evaluated from this data.
© 2002 Elsevier Science B.V. All rights reserved.

Keywords: Plastic bonded explosives; HMX; Thermolysis; Kinetics; Isoconversional method

1. Introduction

Plastic bonded explosives are a type of composite energetic materials in which a high explosive is dispersed (filler) in a polymer (binder) matrix. The basic aim of making a high energetic compound polymer bound is to reduce its sensitivity to hazardous stimuli such as shock, friction, impact, etc., and to achieve mechanical strength and integrity to the shaped explosive charges. Thermal characterization is an essential step in the study of energetic materials. This is because the above-stated hazardous stimuli eventually triggers off a thermal event, which is one of the main causes of initiation of any explosive [1]. Thermal characterization and analysis of energetic materials is important, not only from the point of view of safety and application, but also from the academic point of view. The data from thermal characterization and its kinetic analysis may help in the research efforts in this field, by predicting the safety of the future formulations.

The thermal characterization of potential energetic compounds as filler in plastic bonded explosives (PBXs) such as RDX [2,3], HMX [4,5], NTO [6,7], etc. were the subject of numerous treatises and is well known. The events that are occurring during thermolysis of binder materials for PBXs such as hydroxyl terminated polybutadiene (HTPB) [8–10], polyurethanes [11,12], Kel-F [13], etc. are also available

* Corresponding author. Tel.: +91-551-202856/200745; fax: +91-551-340459.
E-mail address: gsingh4us@yahoo.com (G. Singh).

0040-6031/02/$ – see front matter © 2002 Elsevier Science B.V. All rights reserved.
PII: S0040-6031(02)00460-4

in literature. However, the thermal analysis of PBXs as such is only meagerly available in literature [14]. Although the various establishments, which are involved in the development of PBX formulations, have done routine characterization of the PBXs [15–17], a systematic study on the effect of various additives on the thermal stability and the underlying chemistry of the thermolysis is not yet available in open literature. Some studies are available in literature [18–21] on the thermolysis of nitramine propellants, which are essentially composite energetic materials and very much similar to PBXs. Recently, Chaves et al. [14] have studied the influence of binder (HTPB), plasticiser (bis-2-ethylhexylsebacate, DOS) and curative (isophorone diisocyanate, IPDI) on the thermal decomposition of PBX, based on RDX. They have concluded that although the thermal stability of RDX does not change in the PBX, the additives change the reaction pathways. Singh et al. [22] have showed that plasticisers have no remarkable effect on thermal characteristics of the PBX (RDX-polyurethane). Thermal characterization of PBX containing HMX and HTPB has been reported by Lee and Hsu [23].

We are involved in the thermal analysis of high energetic materials [24] for the last 30 years. As a part of our ongoing program on energetic materials, thermolysis of two PBX formulations based on HMX and polyurethane binder (Estane) has been studied using TG, DSC, DTA and explosion delay techniques. The thermolysis of pure ingredients has also been studied for comparison. Kinetic analysis of the isothermal TG data has been made, both by using the mechanism based kinetic models [25,26] and by using a model free 'standard' isoconversional method [27]. The merits and demerits of both methods have been comparatively analyzed and reported in this paper.

2. Experimental section

Samples of HMX, Estane and two PBX formulations containing HMX and Estane in the ratios 95:5 (HXE 9505) and 90:10 (HXE 9010) have been supplied by TBRL, Chandigarh. Non-isothermal TG–DTG analysis of the samples has been done by using a DuPont 2100 TG instrument at a heating rate of 10 °C min^{-1} (sample mass ≈2 mg, atmosphere = flowing N_2 gas at a rate of 60 ml min^{-1}). DSC analysis on the samples sealed in aluminum pans has been done by using DuPont 2100 DSC instrument at a heating rate of 10 °C min^{-1} (sample mass ≈2 mg, atmosphere = flowing N_2 gas at a rate of 60 ml min^{-1}). Non-isothermal TG analysis has also been made in static air atmosphere at a heating rate of 10 °C min^{-1}, using an indigenously fabricated TG apparatus [28] (sample mass ≈25 mg). DTA analysis of the samples are also carried out in flowing air (60 ml min^{-1}) atmosphere at a heating rate of 10 °C min^{-1}, using a DTA apparatus by Universal Thermal Analysis Instruments, Mumbai. Sample mass was kept as ∼5 mg for HMX and the PBXs, whereas for Estane, it was about 35 mg. Isothermal TG studies of the samples were done at appropriate temperatures using the above-stated indigenously fabricated TG apparatus at static air atmosphere. Approximately 25 mg sample mass has been used for each run. Explosion delay measurements of HMX and the PBXs have been made using tube furnace (TF) technique [29]. The details of the experiments were as reported earlier [30].

3. Results

3.1. TG–DTG and DSC

The TG–DTG thermograms of HMX, HXE 9505, HXE 9010 and Estane are shown in Fig. 1 and the phenomenological data is summarized in Table 1. The results of the TG–DTG analysis of HMX are in agreement with the literature reports [31] and the thermolysis occur in a single rapid step. The TG thermogram of Estane shows that mass loss occurs in a single step at a wide range of temperature (300–400 °C). However, the DTG peak at 379 °C has a shoulder at around 350 °C, which indicates that the thermal decomposition consists of at least two overlapping processes. A careful examination of the TG–DTG data reveals that the onset temperature (T_i) and the endset temperature (T_f) for both the PBX formulations are lower than that for pure HMX. However, the nature of thermograms for the PBXs is more or less similar to that for HMX. Since the thermolysis of the PBXs is occurring in a single and rapid step, it may also be inferred that the decomposition of a considerable amount of the binder is also taking place along with that of HMX.

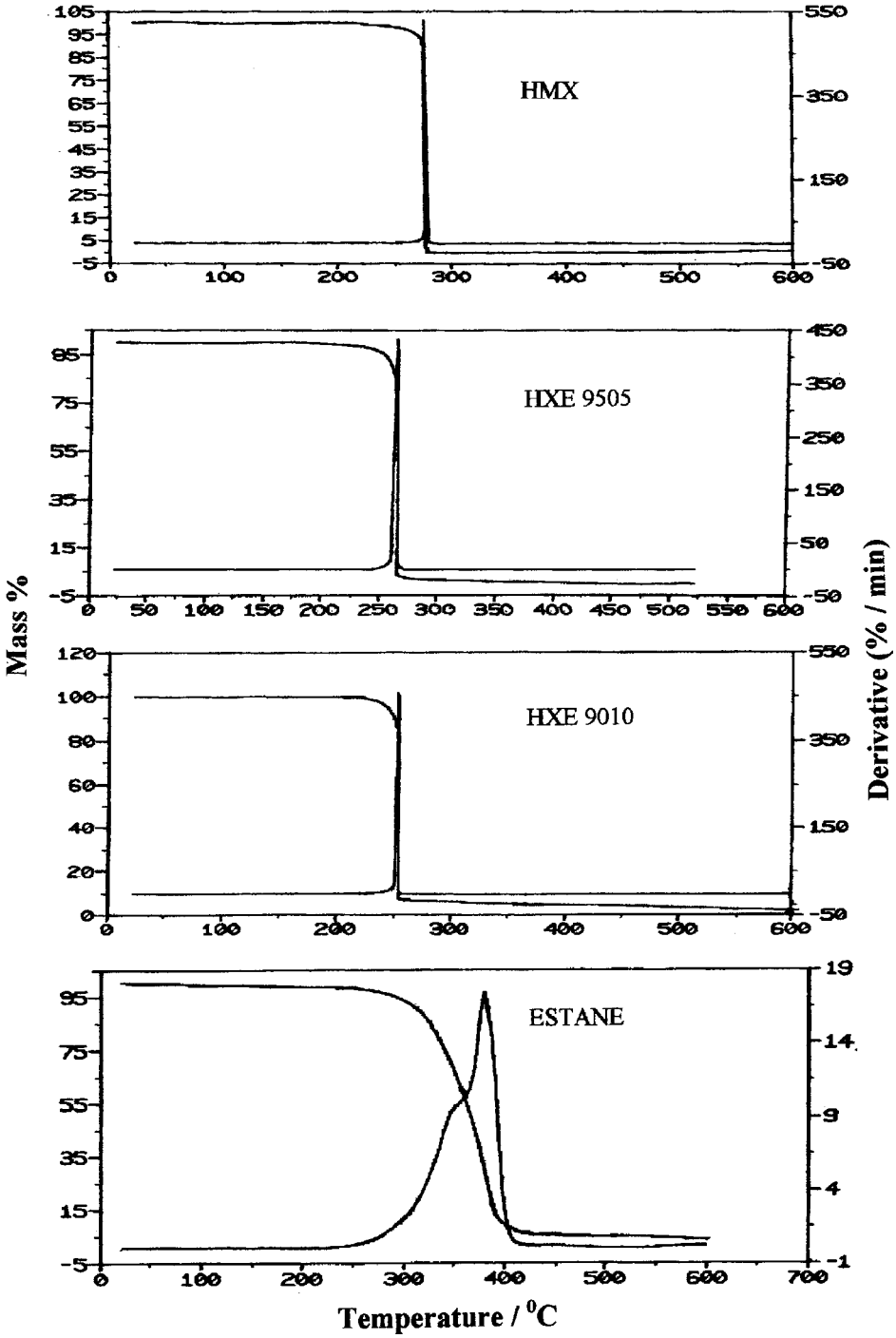

Fig. 1. TG–DTG thermograms of HMX, HXE 9505, HXE 9010 and Estane under inert (N_2) atmosphere.

Table 1
TG–DTG and DSC phenomenological data of HMX, Estane and their PBXs in inert atmosphere

Sample name	TG–DTG		DSC peak temperature (°C)		ΔH (J g^{-1})	
	T_i[a] (°C)	% Decomposition	Endo	Exo	Endo	Exo
HMX	277.7	99.97	186.8	285.9	31.6	1211
Estane	302.1	41.30	223.5	–	6.1	
	377.8	52.66	355.2	–	319.8	–
			390.2	–	–	–
HXE 9505	263.2	97.00	187.4	278.0	28.8	1386
HXE 9010	253.6	94.78	186.4	272.0	25.2	1647

[a] Onset temperature.

An overlay of the DSC thermograms in the temperature range 170–240 °C is shown in Fig. 2a and that in the range 200–450 °C is shown in Fig. 2b. The corresponding data profile is summarized in Table 1. Fig. 2a shows an endotherm in the case of HMX and its PBXs approximately around 186 °C, which is due to the β–α polymorphic transition of HMX [31]. Melting of HMX is reported [4] to be taking place at around 280 °C as per DSC analysis at a heating rate of 10 °C min^{-1}. In our study, the decomposition started at around 278 °C. But a close examination of the DSC peak shows that there is a hump near the onset temperature of the exothermic peak. This may be due to the competition between the melting and decomposition processes while the latter process predominates. The endothermic peak at around 223 °C in case of Estane (Fig. 2a) may be due to the breaking of urethane linkage leading to depolymerisation [11]. The second broad endothermic peak (Fig. 2b) starts at around 260 °C and ends at 420 °C. Fig. 2b and Table 1 reveal that the onset, end set and peak temperatures for exothermic decomposition of HXE 9505 as well as HXE 9010 are considerably lower than those for pure HMX. The extent of lowering increases as the percentage of Estane increases in the PBXs. It is also notable that the enthalpy of these exothermic processes (ΔH) (Table 1) also increases as the percentage of binder increases.

3.2. TG and DTA

In order to determine whether the atmosphere plays any role in the thermolysis of these samples, non-isothermal TG and DTA experiments have been carried out under air atmosphere. The TG thermograms are shown in Fig. 3 and the data profile is summarized in Table 2. The DTA thermograms are shown in Fig. 4 and the corresponding data are summarized in Table 2. The nature of the DSC thermograms and DTA thermograms are essentially the same for HMX and its PBXs, except that the endothermic phase transition peak is absent, due to the low sensitivity of DTA. However, further lowering of exothermic peak temperature is observed for HMX and its PBX samples under reactive atmosphere (DTA), compared to an inert atmosphere (DSC). In the case of Estane, the thermal processes are not clearly revealed in DTA, as the enthalpy involved is very low and hence the data is not reported and will not be discussed further.

3.3. Isothermal TG

Isothermal TG thermograms of HMX, HXE 9505 and HXE 9010 are given in Fig. 5. HMX and HXE 9505 are analyzed in the same temperature range, i.e. 265–280 °C. But in the case of HXE 9010, above 270 °C, the sample cooks-off after a while. Hence, the

Table 2
TG and DTA phenomenological data of HMX, Estane and their PBXs in static air atmosphere

Sample name	TG			DTA peak temperature (°C) (exo)
	SDT[a] (°C)	FDT[b] (°C)	% Decomposed	
HMX	270	305	98	279
Estane	298	400	97	–
HXE 9505	260	290	95	273
HXE 9010	255	280	92	268

[a] Starting decomposition temperature.
[b] Final decomposition temperature.

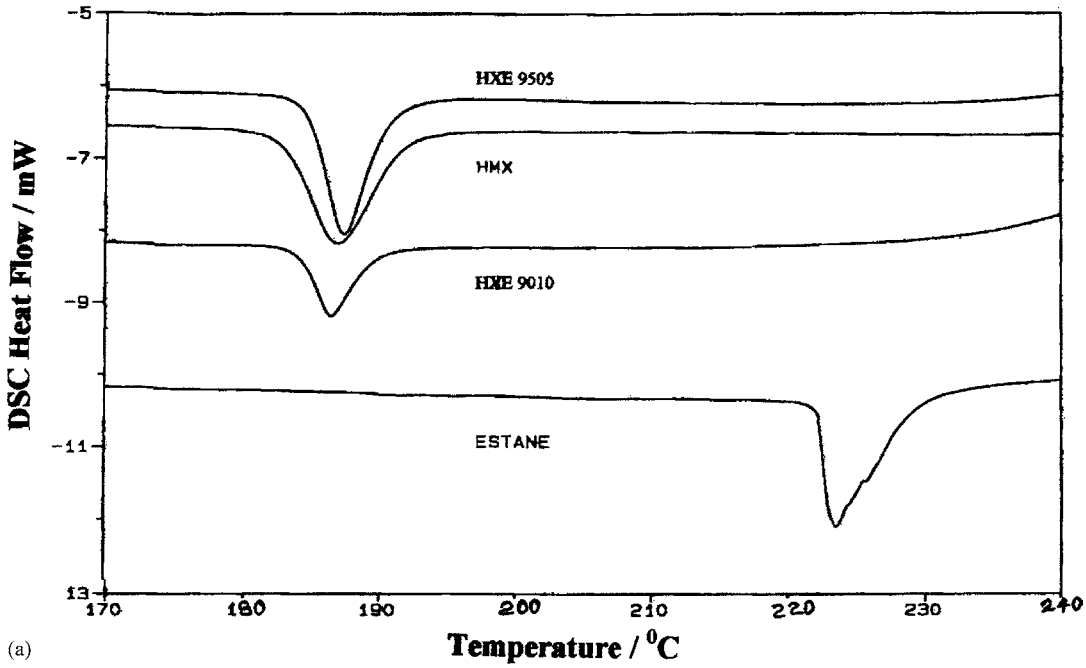

(a)

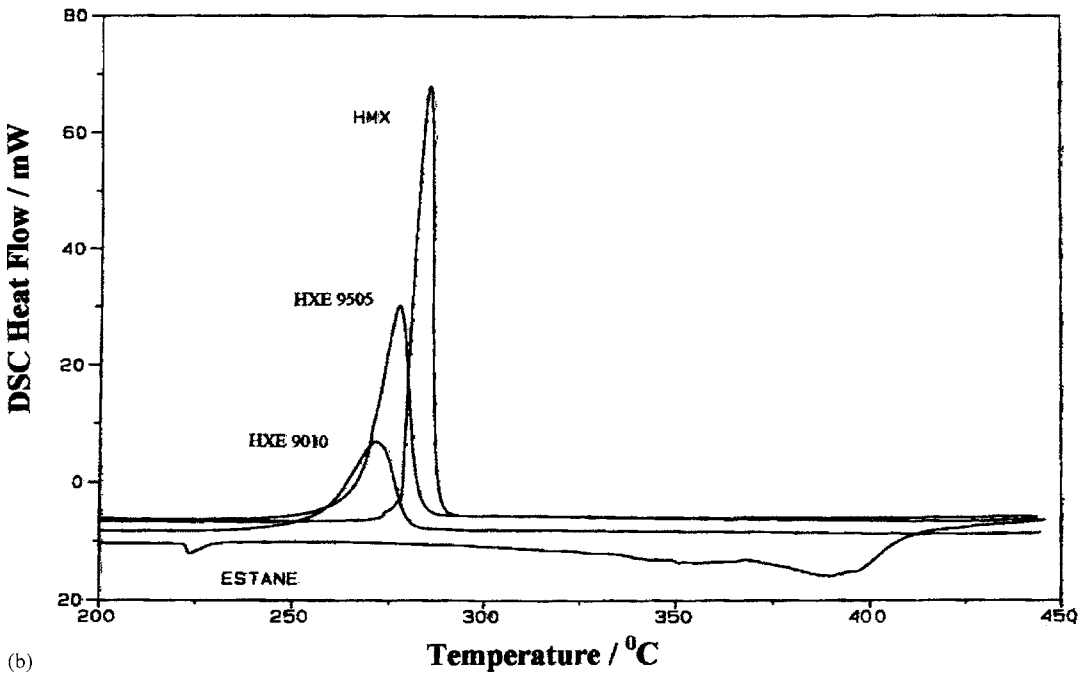

(b)

Fig. 2. DSC thermograms of HMX, HXE 9505, HXE 9010 and Estane under inert (N_2) atmosphere: (a) in the temperature range 170–240 °C and (b) in the temperature range 200–450 °C.

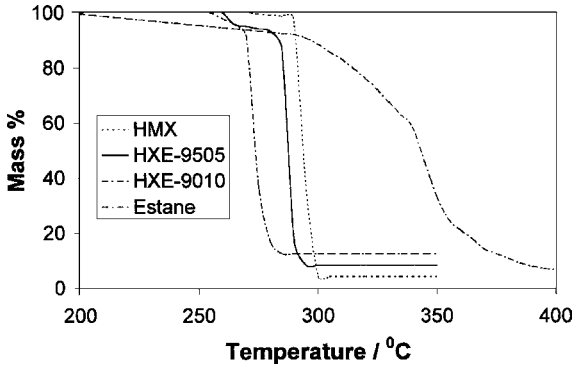

Fig. 3. Non-isothermal TG thermograms of HMX, HXE 9505, HXE 9010 and Estane under static air atmosphere.

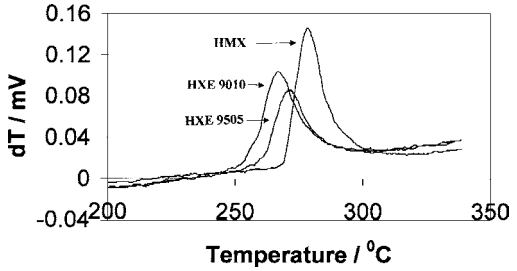

Fig. 4. DTA thermograms of HMX, HXE 9505 and HXE 9010 under flowing air atmosphere.

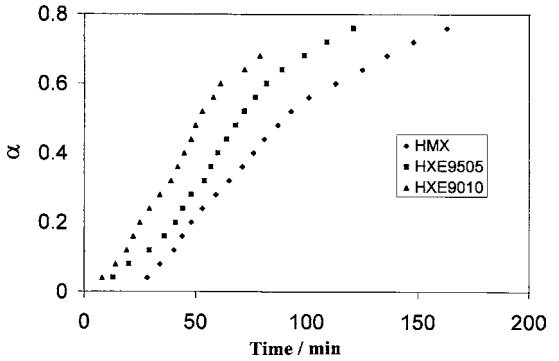

Fig. 6. An overlay of isothermal TG thermograms of HMX, HXE 9505, HXE 9010 and Estane at 270 °C.

isothermal TG studies on this formulation have been made in a lower temperature range, i.e. 255–270 °C. The shape of the thermograms for HMX is sigmoidal in nature as reported in literature [4]. This is true for the PBX samples also. However, an overlay of the data at 270 °C for HMX, HXE 9505 and HXE 9010, given in Fig. 6 shows that thermolysis of PBXs occurs faster than that of pure HMX. Among the PBXs, HXE 9010 decomposes faster than HXE 9505.

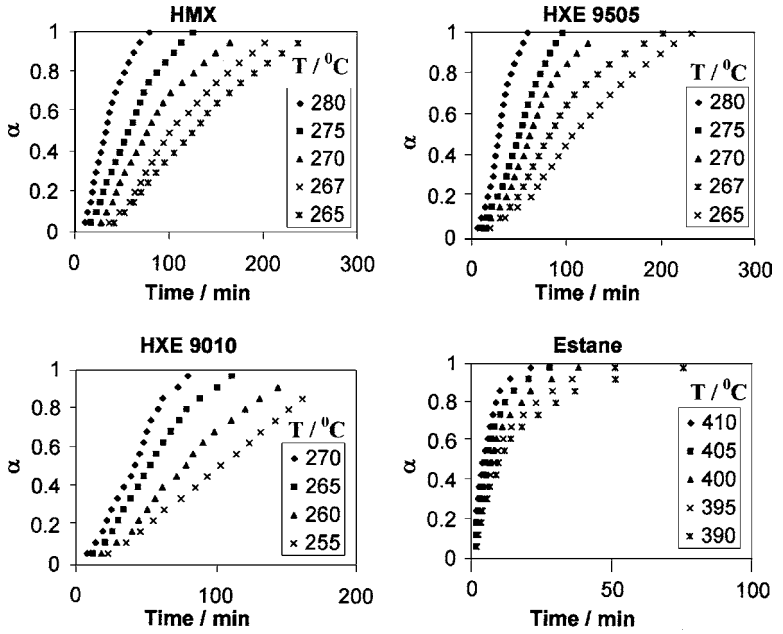

Fig. 5. Isothermal TG thermograms of HMX, HXE 9505, HXE 9010 and Estane.

Table 3
Various mechanism based kinetic models generally used to describe thermal decomposition of solids

S. no.	Model	$f(\alpha)$	$g(\alpha)$
1	Power law	$4\alpha^{3/4}$	$\alpha^{1/4}$
2	Power law	$3\alpha^{2/3}$	$\alpha^{1/3}$
3	Power law	$2\alpha^{1/2}$	$\alpha^{1/2}$
4	Power law	$2/3\alpha^{-1/2}$	$\alpha^{3/2}$
5	One-dimensional diffusion	$1/2\alpha^{-1}$	α^{2}
6	Mampel (first-order)	$1-\alpha$	$-\ln(1-\alpha)$
7	Avrami–Erofeev	$4(1-\alpha)[-\ln(1-\alpha)]^{3/4}$	$[-\ln(1-\alpha)]^{1/4}$
8	Avrami–Erofeev	$3(1-\alpha)[-\ln(1-\alpha)]^{2/3}$	$[-\ln(1-\alpha)]^{1/3}$
9	Avrami–Erofeev	$2(1-\alpha)[-\ln(1-\alpha)]^{1/2}$	$[-\ln(1-\alpha)]^{1/2}$
10	Contracting sphere	$3(1-\alpha)^{2/3}$	$1-(1-\alpha)^{1/3}$
11	Three-dimensional diffusion	$2(1-\alpha)^{2/3}(1-(1-\alpha)^{1/3})^{-1}$	$[1-(1-\alpha)^{1/3}]^2$
12	Contracting cylinder	$2(1-\alpha)^{1/2}$	$1-(1-\alpha)^{1/2}$
13	Prout–Tomkins	$\alpha(1-\alpha)$	$\ln(\alpha/1-\alpha)$
14	Ginstling–Brounshtein	$3/2[(1-\alpha)^{-1/3}-1]^{-1}$	$[1-(2\alpha/3)]-(1-\alpha)^{2/3}$

In the case of Estane, only a small percentage mass loss is observed in the temperature range where the decomposition of HMX has been studied. Therefore, isothermal TG of Estane has been done in the temperature range 390–410 °C and the corresponding thermograms are also given in Fig. 5.

3.4. Kinetic analysis of isothermal TG data

3.4.1. Model fitting method

The basic equation for kinetic evaluation of solid-state thermal decomposition reactions is the well-known expression for rate, which is

$$\frac{d\alpha}{dt} = k(T)f(\alpha) \quad (1)$$

where α is the extent of conversion, t represent time, T the absolute temperature, $k(T)$ the temperature-dependant rate constant and $f(\alpha)$ a function called the reaction model (Table 3). The temperature dependency of rate constant is assumed to obey Arrhenius expression:

$$k(T) = A\exp\left(-\frac{E}{RT}\right) \quad (2)$$

where A is preexponential (Arrhenius) factor, E the activation energy and R the gas constant. Eq. (1) is often used in its integral form, which for isothermal conditions becomes

$$g(\alpha) \equiv \int_0^{\alpha} [f(\alpha)]^{-1}\,d\alpha = k(T)t \quad (3)$$

where $g(\alpha)$ is the integrated form of the reaction model (Table 3). Substituting a particular reaction model into Eq. (3) results in evaluating the corresponding rate constant, which is found from the slope of the plot of $g(\alpha)$ versus t. For each reaction model selected, the rate constants are evaluated at several temperatures and the Arrhenius parameters are evaluated using the Arrhenius equation in its logarithmic form:

$$\ln k(T) = \ln A - \frac{E}{RT} \quad (4)$$

Arrhenius parameters evaluated for the isothermal TG data of HMX, Estane and their PBXs are given in Tables 4–7. The correlation coefficient (r) is usually

Table 4
Arrhenius parameters for isothermal decomposition of HMX

Model[a]	E (kJ mol^{-1})	$\ln A$ (min^{-1})	$-r$
1	197.9	38.14	0.9951
2	198.1	38.39	0.9931
3	198.5	38.70	0.9951
4	200.2	39.41	0.9951
5	201.0	39.57	0.9951
6	202.6	40.94	0.9951
7	199.8	39.05	0.9952
8	200.0	39.38	0.9952
9	200.7	39.88	0.9952
10	201.4	39.16	0.9951
11	204.0	39.21	0.9948
12	200.8	39.27	0.9951
13	200.1	41.03	0.9952
14	202.8	38.49	0.9949

[a] Enumeration of the models are as given in Table 3.

Table 5
Arrhenius parameters for isothermal decomposition of Estane

Model[a]	E (kJ mol^{-1})	ln$A$ (min^{-1})	$-r$
1	261.5	42.19	0.9988
2	260.9	42.30	0.9987
3	259.8	42.37	0.9988
4	254.8	41.92	0.9989
5	253.1	41.67	0.9991
6	252.5	42.83	0.9992
7	256.8	42.06	0.9991
8	256.2	42.22	0.9991
9	255.0	42.43	0.9991
10	253.6	41.36	0.9952
11	251.0	40.60	0.9993
12	254.4	41.65	0.9991
13	256.3	43.92	0.9991
14	251.4	40.05	0.9993

[a] Enumeration of the models are as given in Table 3.

used as a parameter for choosing the best model and the values of which are also reported in Tables 4–7.

3.4.2. Isoconversional method

In isoconversional method, it is assumed that the reaction model in Eq. (1) is not dependant on temperature. Under isothermal conditions, we may combine Eqs. (3) and (4) to get

$$-\ln t_{\alpha,i} = \ln\left[\frac{A}{g(\alpha)}\right] - \frac{E_\alpha}{RT_i} \quad (5)$$

where E_α is evaluated from the slope for the plot of $-\ln t_{\alpha,i}$ against T_i^{-1}. Thus values of E_α for HMX, Estane and PBXs were evaluated at various α_i. The dependencies of activation energy (E_α) on extent of conversion (α) are given in Fig. 7.

Table 6
Arrhenius parameters for isothermal decomposition of HXE 9505

Model[a]	E (kJ mol^{-1})	ln$A$ (min^{-1})	$-r$
1	240.4	47.73	0.9934
2	246.0	47.84	0.9934
3	239.2	47.89	0.9933
4	235.3	47.33	0.9922
5	234.1	47.04	0.9915
6	234.1	48.05	0.9894
7	237.9	47.66	0.9924
8	237.4	47.79	0.9922
9	236.4	47.92	0.9917
10	235.0	46.76	0.9912
11	232.6	45.67	0.9883
12	235.5	47.09	0.9917
13	237.9	49.55	0.9921
14	233.0	45.32	0.9897

[a] Enumeration of the models are as given in Table 3.

Table 7
Arrhenius parameters for isothermal decomposition of HXE 9010

Model[a]	E (kJ mol^{-1})	ln$A$ (min^{-1})	$-r$
1	140.3	26.05	0.9969
2	140.6	26.31	0.9969
3	141.1	26.67	0.9969
4	145.1	27.87	0.9942
5	147.3	28.34	0.9913
6	150.3	30.11	0.9956
7	146.8	28.01	0.9913
8	147.0	28.33	0.9921
9	147.7	28.85	0.9932
10	148.0	28.05	0.9941
11	151.8	28.44	0.9967
12	147.0	28.06	0.9933
13	147.7	30.13	0.9923
14	149.4	27.40	0.9858

[a] Enumeration of the models are as given in Table 3.

3.5. Explosion delay studies

Explosion delay (D_E) at various temperatures for HMX and the PBXs have been measured and the values are summarized in Table 8. The values of D_E were found to obey the following equation [32–34]:

$$D_E = A \exp\frac{E^*}{RT} \quad (6)$$

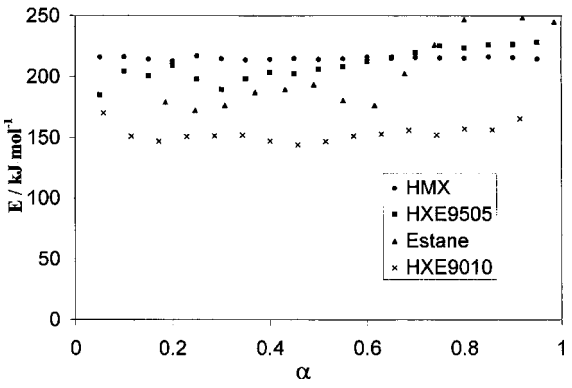

Fig. 7. The dependencies of activation energy (E) on extent of conversion (α) for HMX, HXE 9505, HXE 9010 and Estane, obtained using isoconversional method from the isothermal TG data.

Table 8
Explosion delay (D_E) and activation energy for thermal explosion (E^*) for HMX and its PBXs

Sample	D_E (s) at various temperatures (°C)							E^* (kJ mol^{-1})	r
	300	350	400	450	500	600	690		
HMX	118.00	60.20	45.28	31.33	24.75	17.25	11.15	26.36	0.9947
HXE 9505	105.06	59.47	44.84	30.81	24.06	16.50	11.00	25.65	0.9978
HXE 9010	101.10	55.84	42.21	28.30	23.57	15.70	10.90	25.40	0.9964

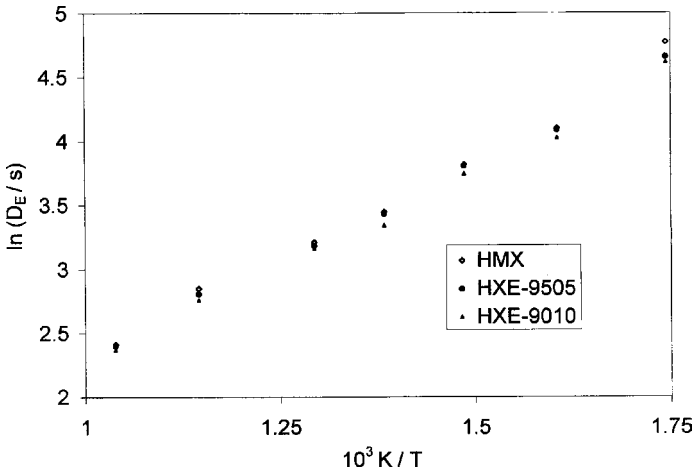

Fig. 8. The plot of $\ln D_E$ versus T^{-1} for HMX, HXE 9505 and HXE 9010.

where E^* is the activation energy for thermal explosion. Eq. (6) is used in its logarithmic form to evaluate E^* from a plot of $\ln D_E$ versus T^{-1}. The plot of $\ln D_E$ versus T^{-1} for HMX and its PBXs are given in Fig. 8 and the values of E^* are summarized in Table 8.

4. Discussion

The results of TG–DTG and DSC studies clearly show that the thermal stability of HMX is at stake when Estane is used as a binder to form corresponding PBX, in the tested conditions. The TG and DTA studies also confirm this apprehension beyond doubt. The extent of lowering in decomposition temperature for HMX increases as the percentage of binder increases. Fig. 2b clearly shows that the exothermic decomposition process in the case of HXE 9010 is almost complete, even before the onset temperature for the thermolysis of pure HMX and it takes place below the melting point of HMX. It is also notable that the enthalpy change (ΔH) (Table 1) for the exothermic decomposition of HMX and its PBXs follows the order HXE 9010 > HXE 9505 > HMX. This may be due to the change in reaction pathways. The gasification of the binder also taking place along with that of HMX, probably due to the high heat release, is evident from the TG–DTG data. If we consider that the decomposition of HMX is complete at the endset temperature in the TG thermograms of the PBXs, then the mass of residue at this temperature must be of binder. In the case of HXE 9505, a residue of 3% (by mass) and for HXE 9010 a residue of 5.2% (by mass) is obtained. Thus we can see that almost 40% of the binder is consumed in the case of HXE 9505 and 48% is consumed in the case of HXE 9010 in the first step itself. The higher percentage consumption of binder in HXE 9010 may be due to the higher heat release. It is also notable that any further mass loss does not occur in the PBXs. This also shows that binder has decomposed in the first step itself and the carbonaceous residue left behind, does not decompose further.

Under the same conditions, the thermal decomposition of Estane is overall endothermic in nature (Fig. 2b). The thermal decomposition of the Estane is reported [11] to be taking place in multi-steps. In the first step, depolycondensation of the urethane linkage takes place, regenerating the diol and isocyanate. The endotherm at around 223 °C, corresponds to this process. However, there is no significant mass loss during this step in TG. Volatilization of the monomers takes place in the next step along with the formation of further byproducts through oxidation–reduction reactions. The volatilization of the products competes with the oxidation–reduction reactions. Under an inert atmosphere, it seems that the former process is the predominant one.

We searched the literature in order to have an explanation for the reduction in the decomposition temperature of HMX in its PBXs, both under inert as well as air atmospheres. Ger et al. [35] reported that when energetic binders such as polyethylene glycol (PEG) and glycidyl azide polymer (GAP) were mixed with RDX and HMX, reduction in decomposition temperature of the pure constituents took place. It has been explained that the exothermic decomposition of the binder, which takes place at a lower temperature than that of the energetic filler, supplies enough heat for the early decomposition of the filler and thus thermal stability of the mixture is lowered [35]. In our case, it should be borne in mind that the thermolysis of Estane is not exothermic overall, under an inert atmosphere. Thus the above-said explanation does not suit for our samples, at least in an inert atmosphere. One possible explanation may be that free radicals, which might have formed during the thermolysis of Estane, interact with HMX and thus cause its early decomposition. In such a case, the mechanism of thermolysis may change, which may be assessed by kinetic analysis. Actually, DSC thermogram (Fig. 2a and b) shows that thermal reactions in Estane start even before the onset temperature of TG. Thus these reactions, which do not lead to gasification, may be having some role in the early decomposition of HMX.

4.1. Kinetic analysis of TG data

Solid-state kinetics may be studied by thermal analysis. Although there is considerable skepticism against solid-state reaction kinetics by thermal analysis, if presented cautiously will give some useful indications of the mechanistic pathways. Model fitting methods are traditionally used for obtaining global activation energies of solid-state thermal decomposition reactions. The data presented in Tables 4–7 show that the generally accepted method of choosing the 'best fit' from the value of correlation coefficient fails in all the four cases. The values of r for various models in the case of a particular sample are either same or very close to each other. At the best, one can eliminate a few models, but to choose a best model solely based on the value of r is a difficult task. It can also be observed from Tables 4–8 that the values of kinetic parameters such as E and $\ln A$ are very close, whatever the form of $g(\alpha)$ used. Thus the value of activation energy obtained for HMX (i.e. approximately 200 kJ mol^{-1}) is a good estimate and is very close to the accepted value [36] of activation energy ($\approx$217 kJ mol^{-1}) for the thermolysis of HMX. The values of activation energy obtained for HXE 9505 is approximately 235 kJ mol^{-1} and is higher than that for HMX, whereas E for HXE 9010 is about 145 kJ mol^{-1}, which is lower. However, the change in values of E is accompanied with a change in frequency factor. A plot of $\ln A$ (min^{-1}) versus E (Fig. 9) reveals that the change in activation energy is accurately compensated by the change in frequency factor, showing 'kinetic compensation effect'. Thus it is very difficult to make any useful interpretation from the kinetic data obtained from model fitting methods.

Many of the disadvantages of the traditional model fitting methods can be overcome by model free isoconversional methods [27,37]. These methods yield

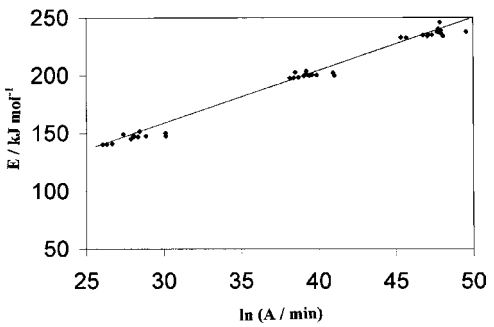

Fig. 9. The plot of E versus $\ln A$ for HMX, HXE 9505 and HXE 9010, showing kinetic compensation effect.

the effective activation energy as a function of extent of conversion and thus assist in detecting multi-step complex reactions. We have adopted the isoconversional method suggested by Vyazovkin [27], since the same method was used in the thermolysis of HMX [4,38] and its composite propellant with HTPB [18]. Lofy and Wight [4] have studied the kinetics of thermolysis of HMX, using non-isothermal TG, isothermal TG, non-isothermal DSC and isothermal DSC and concluded that the global activation energy for thermal decomposition ($146 \pm 14\,kJ\,mol^{-1}$) is independent of extent of conversion. Our kinetic computations for the thermolysis of HMX from the isothermal TG data shown in Fig. 5 agree well with the above-said observation. However, the average activation energy value from our study ($215\,kJ\,mol^{-1}$) differs from their value. This difference might have arose from the fact that in the above-said study, the thermolysis of HMX was studied below its melting point, whereas in our case the temperature range chosen was in the region of melting point of HMX. Thus the results also suggests a difference in mechanism of thermolysis of HMX below its melting point and in/above its melting point.

The results of isoconversional kinetic computations on HXE 9505 and HXE 9010 reveal that the activation energy for thermolysis is independent of extent of conversion, in these cases also. The average value of activation energy for HXE 9505 ($208.4\,kJ\,mol^{-1}$) is almost same as that for pure HMX. However, the average value of E for HXE 9010 ($153.2\,kJ\,mol^{-1}$) is considerably lower than that for HMX. But the decrease in activation energy cannot be attributed to any catalytic decomposition of HMX in HXE 9010. The difference in activation energy is only due to the difference in the range of temperature studied. In fact, the temperature range used for studying the thermolysis of HXE 9010 was lower than the melting point of HMX. Interestingly the value of E for HXE 9010 matches well with the value reported by Lofy and Wight [4] for the thermolysis of HMX from isothermal TG studies, below its melting point. Thus the kinetic parameters from isoconversional computations do not suggest any difference in mechanism of thermolysis of HMX in its PBXs with Estane. The role of binder seems to be reducing the decomposition temperature of HMX, without affecting the energy barrier.

Activation energy of approximately $250\,kJ\,mol^{-1}$ is obtained for the thermal decomposition of Estane, from model fitting methods along with a frequency factor of $42\,min^{-1}$. However, the isoconversional method shows that the activation energy does not remain constant throughout during the thermolysis of Estane (Fig. 7). An average value of E, $181.7\,kJ\,mol^{-1}$ is observed up to around 50% conversion, which gradually changes into $244\,kJ\,mol^{-1}$ afterwards. In fact, DTG shows a change in the value of $d\alpha/dT$ at around 40% conversion and thus isoconversional method clearly reflects the complexity and changes in the mechanism during the thermolysis of Estane.

Further analysis of the gaseous as well as condensed phase reaction products are suggested to study the reason behind the observed lowering in decomposition temperature of PBXs. Such a study could only reveal the actual mechanism of thermolysis and the work is underway in our laboratory and would be reported later on.

4.2. Explosion delay studies

The measurement of explosion delay and evaluating the kinetic parameters there from is an effective method to understand the thermal stability of energetic compounds [34]. It was also used effectively to study the catalytic activity of certain additives on energetic materials [29,39,40]. Therefore, it was thought appropriate to undertake these studies on HMX and its PBXs. The values of D_E for HMX at various temperatures are little bit higher than that for the PBXs (Table 8). The difference is perceivable at lower temperatures, whereas it slowly disappears at high temperatures. The value of E^* for the PBXs does not show any considerable change with that for HMX. E^* must be considered as the barrier to total energy transfer, rather than that for any particular molecular process. Thus from these values, it is reasonable to conclude that the barrier to energy transfer is almost same for HMX and its PBXs. It is also notable that our values of E^* (Table 8) are very close to that obtained by Brill and Brush [41] for HMX ($31.3\,kJ\,mol^{-1}$) using their T-jump/FTIR experiments. They have plotted the time to exotherm data at several temperatures under 2.7 atm Ar and obtained apparent activation energy from the slope of the plot. The similarity of both E^* values show the reliability of our experiment.

5. Conclusions

The thermolysis of HMX takes place at a lower temperature in its PBXs with Estane as binder and the extent of lowering increases as the percentage of binder increases. The lowering of decomposition temperature is associated with increase in heat release. The model fitting approach fails to show any complex reactions that are occurring in the pure compounds as well as the PBXs and it suffers from 'kinetic compensation effect'. The isoconversional method does not show the occurrence of any catalytic decomposition of HMX by the binder decomposition products. The activation energy for thermolysis of HMX, HXE 9505 and HXE 9010 is independent of extent of conversion. However, the isoconversional analysis indicates that the kinetic parameters as well as mechanism for the thermolysis of HMX are different, below and above its melting point. The complexity in the thermolysis of Estane is revealed by the isoconversional method. Analysis of gaseous reaction products and residues of thermolysis of the PBXs is required to understand the actual mechanism of decomposition. The explosion delay measurements also do not show any catalytic decomposition of HMX in its PBXs.

Acknowledgements

Thanks are due to Head, Department of Chemistry, for laboratory facilities. Financial support from DRDO, New Delhi is also gratefully acknowledged. Director, TBRL, Chandigarh is thanked for HMX as well as PBX samples. Prof. G.N. Mathur, Director, Dr. D.K. Setua, Joint Director, Mr. Amitabh Chakraborthy and Mr. Y.N. Gupta all of DMSRDE, Kanpur are also thanked for the TG–DTG and DSC data.

References

[1] C.B. Storm, J.R. Stine, J.F. Kramer, Sensitivity Relationship in Energetic Materials in Chemistry and Physics of Energetic Materials, Kluwer Academic Publishers, Dordrecht, 1990, pp. 605–639.
[2] R.N. Rogers, L.C. Smith, Thermochim. Acta 1 (1970) 1.
[3] Y. Oyumi, Propell. Explos. Pyrot. 13 (1988) 42.
[4] P. Lofy, C.A. Wight, Thermal Decomposition of HMX Below its Melting Point, Personal communication.
[5] T.B. Brill, R.J. Kasperowicz, J. Phys. Chem. 86 (1982) 4260.
[6] G. Singh, I.P.S. Kapoor, S.K. Tiwari, P.S. Felix, J. Hazard. Mater. B 81 (2001) 67.
[7] K.V. Prabhakaran, S.R. Naidu, E.M. Kurian, Thermochim. Acta. 241 (1993) 199.
[8] K.N. Ninan, K. Krishnan, R. Rajeev, G. Viswanathan, Propell. Explos. Pyrot. 21 (1996) 199.
[9] J.K. Chen, T.B. Brill, Combust. Flame 87 (1991) 217.
[10] D. Tigfa, Thermochim. Acta 138 (1989) 189.
[11] N. Grassie, A. Gilberto, M. Perdomo, Polym. Degrad. Stabil. 11 (1985) 359.
[12] D. Basal, P.P. De, G.B. Nando, Polym. Degrad. Stabil. 65 (1999) 47.
[13] S.L. Madorsky, S. Straus, J. Res. Natl. Std. 55 (1955) 223.
[14] F. Chaves, J.C. Gois, P. Simoes, in: Proceedings of the 27th International Pyrotechnique Seminar, 2000, p. 865.
[15] M.S. Campbell, D. Garcia, D. Idar, Thermochim. Acta 357–358 (2000) 89.
[16] A.S. Tompa, R.F. Boswell, Thermochim. Acta 357–358 (2000) 169.
[17] M. Lal, S.R. Nayak, R. Narang, S.N. Singh, J. Armt. Stud. XXVII (2) (1992) 142.
[18] G.D. Peterson, C.A. Wight, in: Proceedings of the 28th NATAS Annual Conference on Therm. Anal. Appl., 2000, p. 121.
[19] Y. Oyumi, K. Inokami, K. Yamazaki, K. Matsumoto, Propell. Explos. Pyrot. 18 (1993) 62.
[20] M.W. Beckstead, Pure Appl. Chem. 65 (1993) 297.
[21] Y.J. Lee, C.J. Tang, T.A. Litsinger, Combust. Flame 117 (4) (1999) 795.
[22] S.N. Singh, S.S. Samudra, J.S. Gharia, in: Proceedings of the Second International Autumn Seminar on Propellants, Explosives and Pyrotechniques, 1997, p. 112.
[23] J.S. Lee, C.K. Hsu, in: Proceedings of the 28th NATAS Annual Conference on Therm. Anal. Appl., 2000, p. 383.
[24] http://www.quicksitebuilder.cnet.com/singhgurdip/drgurdip-singh/.
[25] M.E. Brown, D. Dollimore, A.K. Galway, Reactions in Solid State, Comprehensive Chemical Kinetics, vol. 22, Elsevier, Amsterdam, 1980.
[26] J. Sestak, Thermophysical properties of solids, Comprehensive Analytical Chemistry, vol. 12D, Elsevier, Amsterdam, 1984.
[27] S. Vyazovkin, Thermochim. Acta 355 (2000) 155.
[28] G. Singh, R.R. Singh, Res. Ind. 23 (1978) 92.
[29] G. Singh, I.P.S. Kapoor, S.K. Vasudeva, Indian J. Technol. 29 (1991) 589.
[30] G. Singh, I.P.S. Kapoor, J. Phys. Chem. 96 (1992) 1215.
[31] B. Suryanarayana, Graybush, R. Ind. Chim. Belge. 32 (1967).
[32] N. Semenov, Chemical Kinetics and Chemical Reactions, Clarendon Press, Oxford, 1935, Chapter 2.
[33] E.S. Freeman, S. Gordon, J. Phys. Chem. 60 (1956) 867.
[34] J. Zinn, R.N. Rogers, J. Phys. Chem. 66 (1962) 2646.
[35] M.D. Ger, W.H. Hwu, C.C. Huang, Thermochim. Acta 224 (1993) 127.

[36] B.M. Dobratz, LLNL Explosive Handbook: Properties of Chemical Explosives and Explosive Stimulants, UCRL-52997, 1988, p. 6.
[37] M.E. Brown, M. Maciejewski, S. Vyazovkin, R. Nomen, J. Sempere, A. Burnham, J. Opfermann, R. Strey, H.L. Anderson, A. Kemler, R. Keuleers, J. Janssens, H.O. Desseyn, C.R. Li, T.B. Tang, B. Roduit, J. Malek, T. Mitsuashi, Thermochim. Acta 355 (2000) 125.
[38] S. Vyazovkin, C.A. Wight, Thermochim. Acta 340–341 (1999) 53.
[39] G. Singh, I.P.S. Kapoor, J. Energy Mater. 11 (1994) 293.
[40] G. Singh, P.S. Felix, Combust. Flame (2002), in press.
[41] T.B. Brill, P.J. Brush, Phil. Trans. R. Soc. Lond. A 339 (1992) 377.